

## Article

# Improved Representation of Groundwater–Surface Water Interactions Using SWAT+*gwflow* and Modifications to the *gwflow* Module

Estifanos Addisu Yimer <sup>1,\*</sup>, Ryan T. Bailey <sup>2</sup>, Lise Leda Piepers <sup>1</sup>, Jiri Nossent <sup>1,3</sup> and Ann Van Griensven <sup>1,4</sup><sup>1</sup> Department of Hydrology and Hydraulic Engineering, Vrije University of Brussels, 1050 Brussels, Belgium<sup>2</sup> Department of Civil and Environmental Engineering, Colorado State University, Fort Collins, CO 80523, USA<sup>3</sup> Flanders Hydraulics Research, 2140 Antwerp, Belgium<sup>4</sup> Department of Water Science and Engineering, IHE Delft Institute for Water Education, 2700 Delft, The Netherlands

\* Correspondence: estifanos.addisu.yimer@vub.be

**Abstract:** Recent water availability and scarcity problems have highlighted the importance of surface–groundwater interactions. Thus, groundwater models are coupled with surface water models. However, this solution is complex, needing code modifications and long computation times. Recently, a new groundwater module (*gwflow*) was developed directly inside the SWAT code to tackle these issues. This research assesses *gwflow*'s capabilities in representing surface–groundwater system interactions in the Dijle catchment (892.54 km<sup>2</sup>), a groundwater-driven watershed in Belgium. Additional developments were made in SWAT+*gwflow* to represent the interaction between the groundwater and soil (*gwsoil*). The model was calibrated for monthly mean streamflow at the catchment outlet (1983 to 1996) and validated for two periods (validation 1: 1975 to 1982 and validation 2: 1997 to 2002). It was found that the SWAT+*gwflow* model is better at representing the total flow (NSE of 0.6) than the standalone SWAT+ (NSE of 0.4). This was confirmed during two validation periods where the standalone model scored unsatisfactory monthly NSE (0.6 and 0.1), while the new model's NSE was 0.7 and 0.5. Additionally, the SWAT+*gwflow* model simulations better depict the groundwater via baseflow and attain proper water balance values. Thus, in a highly groundwater-driven catchment, the simplified representation of groundwater systems by the standalone SWAT+ model has pitfalls. In addition, the modification made to the *gwflow* module (*gwsoil*) improved the model's performance, which, without such adjustment, overestimates the streamflow via saturation excess flow. When including the *gwsoil* mechanism, thereby providing a more accurate representation of water storage and movement, groundwater is transferred to the soil profile, increasing the overall soil water content and thereby increasing lateral flow. This novel modification can also have implications for other distributed hydrological models to consider such exchanges in their modeling scheme.



**Citation:** Yimer, E.A.; Bailey, R.T.; Piepers, L.L.; Nossent, J.; Van Griensven, A. Improved Representation of Groundwater–Surface Water Interactions Using SWAT+*gwflow* and Modifications to the *gwflow* Module. *Water* **2023**, *15*, 3249. <https://doi.org/10.3390/w15183249>

Academic Editor: Adriana

Bruggeman

Received: 20 July 2023

Revised: 8 September 2023

Accepted: 10 September 2023

Published: 12 September 2023

**Keywords:** ground–surface water interaction; groundwater–soil interaction; geohydrological modeling; inter-model comparison; SWAT+; *gwflow*; Dijle; Belgium



**Copyright:** © 2023 by the authors. Licensee MDPI, Basel, Switzerland. This article is an open access article distributed under the terms and conditions of the Creative Commons Attribution (CC BY) license (<https://creativecommons.org/licenses/by/4.0/>).

## 1. Introduction

Geohydrological systems can be modeled using either surface water, groundwater, or coupled models [1]. However, separate representation of surface and groundwater processes has limitations, as it neglects the interaction between these vital processes [2]. This interlink is essential for the sustainable existence of surface water bodies [3], and in some studies it accounts for the vast majority of the hydrological cycle [4]. This led to an extensive coupling approach to understand the mechanism whereby these two separate but interlinked systems operate [5–8]. For example, the assessment of surface–groundwater interaction in an Alpine valley in Italy indicated that the recharge and pumping of water can be mainly driven by the interaction at the river bed [9]. Therefore, as new challenges

arise regarding water quantity and quality, together with many other water management practices, a more holistic approach towards hydrological modeling is necessary [10–15]. For example, to make accurate forecasts regarding the effects of different drought types [16], water resources should be quantified by holistic models, including both groundwater (GW) and surface water (SW) processes, instead of modeling them separately [17]. This results in modeling concepts where additional modules are implemented in existing code to include GW–SW exchange processes.

The number of models that have both GW and SW modeling schemes has increased over the past 20 years. This coupling of surface water and groundwater is often challenging because of the high spatial and temporal variability between the resulting exchange fluxes [11,18]. An example of a coupled GW–SW flow model is the GSFLOW model by Markstrom et al. [19]. This integrated hydrological model links the Precipitation Runoff Modeling System (PRMS), as the surface water model, with Modular Groundwater Flow (MODFLOW-2005) as a model for the subsurface processes.

Hydrological models such as the Soil and Water Assessment Tool (SWAT) can account for the groundwater component of the hydrological system within the aquifer module, but with important limitations. Like other processes in SWAT, the groundwater head is calculated at the hydrologic response units (HRU) level; hence, the water table is not spatially distributed. Hydraulic conductivity and specific yield do not vary spatially, as each aquifer system is assumed to be homogenous. Therefore, SWAT is not suited to simulating the spatiotemporal variation of groundwater variables. Another limitation is that the groundwater head only changes with recharge and return flow, whereas many other groundwater flows exist (e.g., groundwater extraction through pumping). In addition, return flow is calculated only for steady-state conditions. This component only occurs when groundwater storage surpasses a certain threshold, while in reality this is determined by hydraulic gradients. Also, seepage caused by hydraulic gradients is not simulated [20–22]. Due to these reasons, and since the standalone SWAT model has major limitations for applications on groundwater-dominated catchments [23–27], there has been an intense effort to replace this simplified representation of groundwater hydrology in SWAT.

This led to the coupling of SWAT and MODFLOW [17,18,21,28–30]. The coupled SWAT–MODFLOW framework combines the SWAT software modeling tool with MODFLOW [31], where the latter is embedded as a subroutine, replacing the groundwater module in SWAT. The main issue with integrating SWAT and MODFLOW is the complex model code modification and long computation time requirement. Due to this, Bailey et al. (2020) recently developed a new physical-based groundwater flow module (*gwflow*) as part of the SWAT+ modeling code. SWAT+ is the new and restructured version of SWAT [32]. The *gwflow* module is based on the Dupuit–Forchheimer assumption of horizontal flow in unconfined aquifers. Therefore, this module should be used in cases where the groundwater system is composed of an unconfined aquifer. Hence, this module could replace the current SWAT+ aquifer module for unconfined aquifers and allow for spatially distributed groundwater simulations such as groundwater head (i.e., water table elevation), groundwater storage, groundwater discharge to streams, etc.

However, one critical limitation of the *gwflow* module is that groundwater–soil interactions are not represented, leading to incorrect water balance at the HRU level. These are vital interactions whenever the water table is higher than the bottom of the soil profile. Hence, in this paper, this limitation/research gap is assessed, the source code of the coupled SWAT+*gwflow* model is modified, and a comparison before and after applying this modification is presented. Furthermore, we aimed to apply the coupled model (SWAT+*gwflow*) to a groundwater-influenced catchment located in a temperate climate and investigate how the baseflow is represented. Subsequently, a model output comparison was performed between the standalone SWAT+ and the one modified with the *gwflow* module.

## 2. Materials and Methods

### 2.1. Study Area

Located in the center of Belgium, the Dijle catchment (Figure 1) has an average length of 86 km and an area of 892.54 km<sup>2</sup>. It is a part of the larger Scheldt Basin (21,863 km<sup>2</sup>), situated in Belgium, France, and the Netherlands. The Dijle River springs near Houtain-Le-Val in Wallonia and flows towards the northeast. In Court-Saint-Etienne, the Thyle and Orne Rivers are added to its river flow. In addition, the Train River originating from Wallonia ends up in the Dijle. At the border between Flanders and Wallonia, the Dijle has an average flow rate of 4.5 m<sup>3</sup>/s.

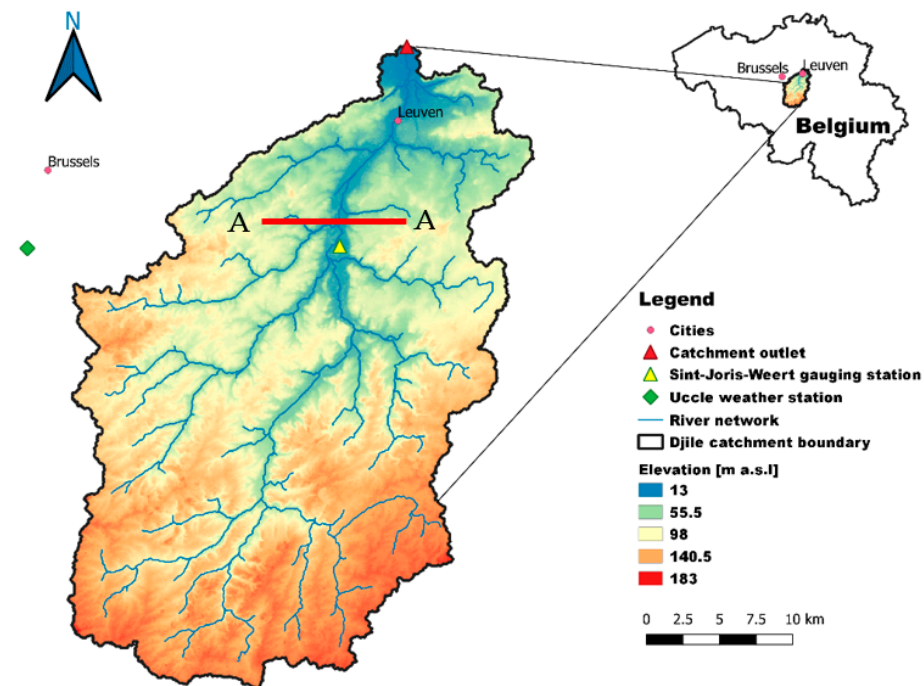


**Figure 1.** Study area map where the catchment outlet is located at Wilsele. The catchment is low land in the northern part and higher in the southern region. The cross-sectional view of section A-A can be found in Figure 2.

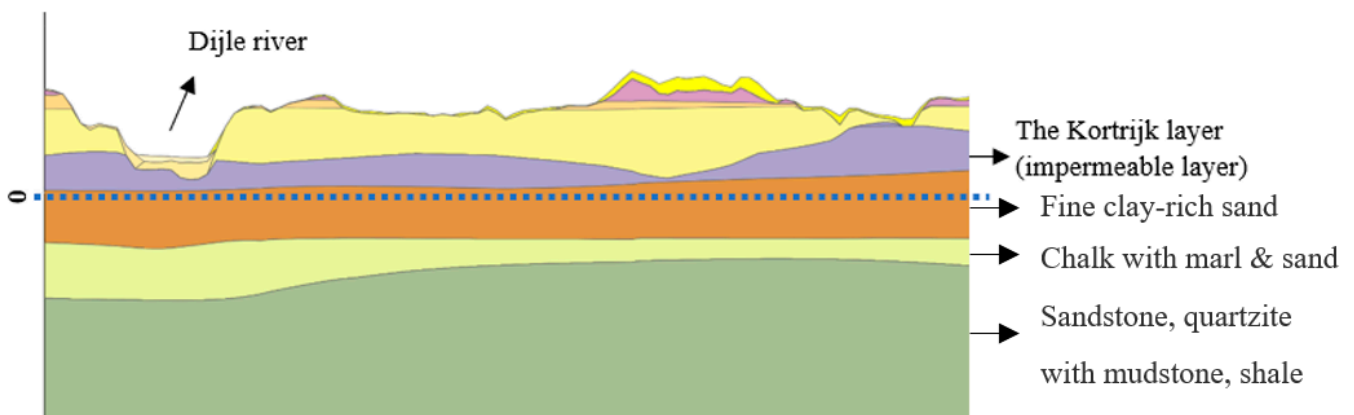


**Figure 2.** The elevation of the impermeable layer base was taken as a reference for the unconfined aquifer. It can be found at <https://www.dov.vlaanderen.be/portaal/>, accessed on 30 September 2021. The other colors correspond to different geological units; however, the focus of this study lies on the impermeable layer and the yellow unit (Brussel sand), which corresponds to the unconfined aquifer. The dotted line corresponds to mTAW = National Topographic Reference). The plot is not to scale, and the transect is for A-A, as seen in Figure 2.

In general, the catchment is homogeneous in terms of soil type, with more than 90% covered by silt-textured Luvisols [33]. Substantial soil textures that can be found in the Dijle catchment include silt, sandy loam, and loamy sand. The area is known to have a spatial transition in texture from northwest to southeast, giving a pattern of sand and sandy loam in the northern part and silt regions in the southwestern part. The sandy aquifer (traditionally known as “Brussels sand”) is dominant, with a lower impermeable layer called Kortrijk, which acts as the base of the unconfined aquifer (Figure 2). The Dijle catchment has a mean elevation of 40 m and an average slope of 2% [34].

The weather data were obtained from the Royal Meteorological Institute of Belgium (RMI) for variables such as precipitation (mm), relative humidity (decimal fraction), solar radiation ( $\text{MJ}/\text{m}^2$ ), temperature ( $^{\circ}\text{C}$ ), and wind speed (m/s) from 1970 until 2011 at the Uccle gauging station. Although this weather station is not situated inside the catchment area, the weather data could be used for this study, as the weather variables are approximately constant spatially across Belgium (refer to Supplementary Materials Figure S1). The average precipitation from a gridded dataset (10 points inside the watershed) indicated similar daily average precipitation values to those measured at the Uccle station (this is also shown on a scatterplot). By the time this research was conducted, the gridded dataset was not available; hence, the Uccle station weather data were used. The other inputs for developing the SWAT+ model were soil and land-use maps obtained from the Food and Agriculture Organization (FAO, Rome, Italy, 2010) and the European Space Agency (ESA, Paris, France, 2020, resolution: 200 m), respectively. Finally, a digital elevation model (DEM) of 50 m by 50 m was reassembled from a 90 m by 90 m DEM acquired from the USGS (<https://earthexplorer.usgs.gov/>, last accessed on 30 September 2021) and used to delineate the catchment. The streamflow data run from 1975 to 2002 for both the catchment outlet (Wilsele) and the Sint-Joris-Weert (SJW) gauging station.

## 2.2. Methodology

The methodology comprised two main parts: the first was modeling the catchment with the standard SWAT+ model, and the second was to use the new “*gwflow*” module as a replacement for the simplistic representation of the groundwater module in the SWAT+ model. This enabled us to assess the potential of the new module (*gwflow*) to simulate the groundwater hydrology of the Dijle catchment better than the standalone model.

### 2.2.1. SWAT+ Model Setup

SWAT+ is an entirely revised version of the Soil and Water Assessment Tool [35], which has been under continuous development since the early 1990s [32]. It is open-source software that was developed to solve water resource management issues [35]. The model is a continuous, semi-distributed, physical-based model that divides the watershed into sub-basins, which are identified based on a topographic map. Each sub-basin can be further subdivided into landscape units (LSUs), which is one of the principal improvements in the development of SWAT+ from SWAT [36]. This option facilitates the inclusion of riparian and floodplain components and improves the runoff-routing capabilities within the landscape. Other adjustments include the flow and pollutant routing throughout the landscape.

These LSUs are further separated into unique combinations of land use, soil, and slope called hydrologic response units (HRUs). At this level, most SWAT+ processes take place (i.e., hydrology, erosion, nutrient cycling, pesticide dynamics, and agricultural management). Flow at the HRU level is summed at the LSU level and then routed to other spatial objects, such as an LSU, channel, wetland, pond, reservoir, or aquifer.

As precipitation reaches the soil surface, it may infiltrate and percolate through it, while evaporation losses occur simultaneously. Part of the water will percolate into the soil and become recharge for the shallow aquifer, further contributing to the streamflow [37]. When the water seeps deeper, it becomes recharge for the deep aquifer and is assumed to contribute to streams outside the watershed. Different methods have been implemented in

SWAT+ to calculate these fluxes [38]. Flow from the shallow aquifer that ends up in streams is referred to as groundwater flow, baseflow, or return flow.

As mentioned above, the groundwater system in SWAT+ can be divided into shallow and deep aquifers. Recharge results from percolation moving through the vadose zone towards the shallow and/or deep aquifer. An exponential decay weighting function (Equation (1)) accounts for the time delay caused by the time needed for the water to leave the soil profile and penetrate the shallow or deep aquifer (Equation (2)). The recharge on a specific day can be estimated with

$$w_{rchrg,i} = \left[ 1 - \exp\left(\frac{-1}{\delta_{gw}}\right) \right] \times w_{seep} + \exp\left(\frac{-1}{\delta_{gw}}\right) \times w_{rchrg,i-1} \quad (1)$$

where  $w_{rchrg,i}$  is the recharge volume moving into the aquifer on day  $i$ ,  $\delta_{gw}$  is the delay time (days),  $w_{seep}$  is the total volume of water leaving the soil profile on day  $i$ , and  $w_{rchrg,i-1}$  is the recharge volume entering the aquifer on day  $i - 1$ . It is not possible to directly measure  $\delta_{gw}$ ; therefore, it should be calibrated. The fraction of water recharging the deep aquifer on a specific day can be calculated by

$$w_{deep,i} = \beta_{deep} \times w_{rchrg,i} \quad (2)$$

where  $w_{deep}$  is the volume of water flowing to the deep aquifer on day  $i$ ,  $\beta_{deep}$  is the aquifer percolation coefficient, and  $w_{rchrg}$  is the recharge volume entering the shallow and deep aquifer on day  $i$ .

The relation used to estimate the baseflow is a function of recharge and the baseflow recession constant  $\alpha_{gw}$ , which is a direct index of the groundwater flow's response to changes in recharge. Values between 0.1 and 0.3 indicate a slow response, while values of 0.9–1.0 characterize a fast response. Baseflow can only enter the stream if a threshold of water present in the shallow aquifer is exceeded, and this threshold is user-defined [38]. Another flow,  $R_{evap}$ , moves from the shallow aquifer towards the covering unsaturated layer during dry periods. In such periods, water from the capillary fringe will evaporate and be replaced by water from the underlying aquifer.  $R_{evap}$  can only occur at baseflow when the water present in the shallow aquifer exceeds a user-defined threshold [38].

The SWAT+ model setup started by delineating the catchment, where the Wilsele gauging station was taken as the catchment outlet, and this resulted in a total catchment area of 892.54 km<sup>2</sup>, with 1496 HRUs, 21 sub-basins, and 162 channels. The streamflow data at Wilsele were downloaded from Waterinfo (<https://www.waterinfo.be/>, last accessed on 21 September 2022) for the same time window as the other weather inputs. The Penman–Monteith equation was chosen as the potential evapotranspiration (PET) calculation method, whereas the Muskingum method was selected for flow routing. We used SWAT+ version 60.5.2 for the model setup.

### 2.2.2. SWAT+ Model with the *gwflow* Module Setup

The original *gwflow* module [20] simulates groundwater fluxes, including lateral flow within the aquifer, recharge for HRUs, evapotranspiration (ET) from shallow groundwater, pumping, interactions between groundwater and surface water through the streambed (i.e., groundwater discharge to streams and seepage to the aquifer), and saturation excess flow. To use the *gwflow* module, the model domain is discretized horizontally in square grid cells (for this research, we used 200 m by 200 m), with each cell representing a volume of aquifer. The module calculates a water balance equation for each grid cell through a control volume method based on mass conservation. For each simulation timestep, Equation (4) is solved for the groundwater volume and correlated groundwater head. These values are calculated explicitly, based on the head values of neighboring grid cells, along with flow from sources and sinks at the preceding timestep. Necessary data for each grid cell include ground surface elevation, aquifer thickness, hydraulic conductivity (m/day), and specific

yield (refer to Supplementary Materials Tables S1 and S2 for the parameters used for the model setup). Each cell must also be analyzed spatially for interactions with streams.

As *gwflo*w is embedded as a subroutine within the SWAT+ Fortran code, the inputs for the standalone SWAT+ model are also inputs for the *gwflo*w model setup. For the SWAT+*gwflo*w module, SWAT+ version 60.5.2 is coupled with the *gwflo*w module. In addition, an aquifer thickness raster (vertical distance from the ground surface to bedrock, i.e., the thickness of unconsolidated sediments) was downloaded from <https://data.isric.org/> (Shangguan et al. [39], last accessed on 21 September 2022). To check the validity of the global dataset, the depth to the impermeable layer, called the Kortrijk layer (Figure 2), was also taken from a previous study conducted by Wossenyeleh, (2021) [40]. The permeability of the aquifer material was obtained from <https://dataverse.scholarsportal.info/> (Huscroft et al., 2018 [41], last accessed on 21 September 2022). This helped us to classify the aquifer into distinct zones, where each zone has its own corresponding hydraulic conductivity ( $K_{aqu}$ ) and specific yield ( $S_y$ ) values [20].

It is worth noting that the global datasets that we used to prepare the *gwflo*w inputs have a mismatch with the locally available data. Hence, we made simplifications to ease the sensitivity and calibration process. For instance, the number of different hydraulic conductivity zones according to the global dataset is 24; however, previous studies on this catchment [42] have shown the dominance of one zone (called “Brussels sand”), and we also noticed from the global dataset that the hydraulic conductivity values for most zones were similar (refer to Supplementary Materials Table S3). Hence, we calibrated only the dominant zones (Figure 3). If we take the 24 zones as independent zones, we would need to perform sensitivity analysis for 24 zones (a total of 48 parameters: 24 for hydraulic conductivity and 24 for specific yield). Note that this number does not account for the other model parameters. This would increase the computation time, create difficulty when calibrating the model at the latter stages, and may lead to overfitting. However, this simplification would not reduce the model’s performance, which is checked at later stages, as described in the Results section. This type of simplification is well-known in hydrological modeling as a parsimonious representation [43–46].

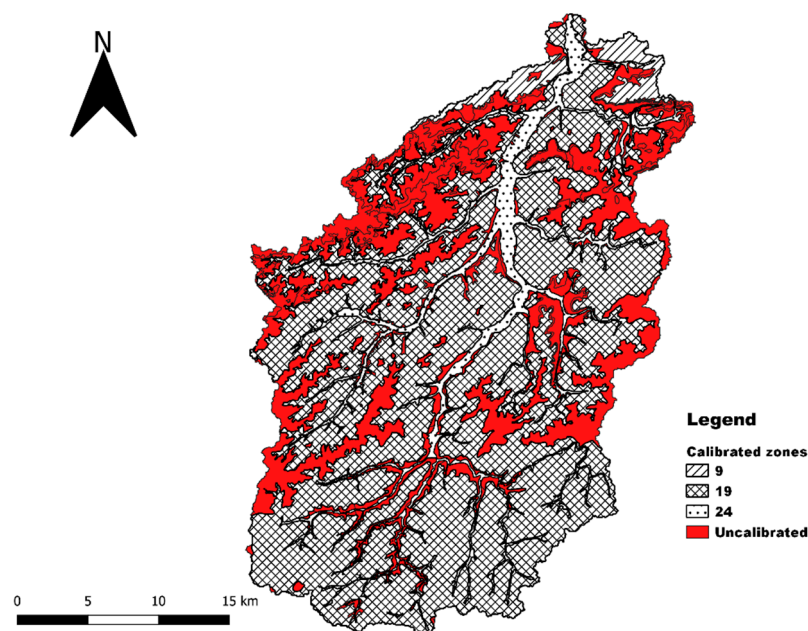


**Figure 3.** The different hydraulic conductivity zones according to the GLHYMS dataset. Originally, there were 24 zones, with 3 dominant zones. Hence, to reduce the computation time and avoid overfitting, only these 3 zones’ hydraulic conductivity and specific yield parameters were calibrated.

### 2.2.3. Modification to the *gwflow* Module

In the original water balance equation of the *gwflow* module [20], the interaction between SWAT+ HRU soil profiles and *gwflow* grid cells occurs only through the passing of deep percolation from the soil profile to groundwater, i.e., the water table elevation—and corresponding groundwater storage—simulated for each grid cell does not interact with or affect the hydrological processes of the soil profile. This could lead to situations where the *gwflow* module simulates a water table within the soil profile, with all inherent groundwater calculations (such as lateral flow), while at the same time, the HRU in the same vicinity as the grid cell is simulating percolation and soil lateral flow. This leads to duplicate processes, but by different equations. To remedy this flaw, in this study, we modified the *gwflow* module to allow the transfer of groundwater to the soil profile for grid cells where the water table rises into the soil profile (Equation (3)). This is particularly important for groundwater-dominated catchments (i.e., high-baseflow fractions) where the water table is shallow. For each cell, for each timestep, the simulated water table elevation (i.e., groundwater head) is compared to the elevation of the soil profile bottom of the HRU to which it is connected spatially. If the water table elevation  $wt_{elev}$  (m) is above the elevation of the soil profile's bottom  $soil_{elev}$  (m), then the volume of groundwater to transfer to the soil profile  $Q_{gw \rightarrow soil}$  can be calculated as follows:

$$Q_{gw \rightarrow soil} = (wt_{elev} - soil_{elev}) \times A_{hru} \times S_y \quad (3)$$

where  $A_{hru}$  is the area (m<sup>2</sup>) of the HRU within the spatial area of the grid cell, and  $S_y$  is the specific yield of the aquifer. This volume of water is added to the HRU soil layers that are at or below the elevation of the water table. The inclusion of this transfer term can yield higher rates of recharge during a model simulation, due to water added to the soil profile that can subsequently move downward to the water table. Therefore, when presenting and discussing model results or estimating recharge rates for a watershed or portion of a watershed, the “net” recharge should be estimated by subtracting the transfer volume from the simulated recharge volume, i.e., true recharge =  $Q_{rech} - Q_{gw \rightarrow soil}$ .

We further modified the module to include municipal pumping, which was added as another sink term in the water balance equation. The start and end dates of pumping and the daily pumping rate are inputs for wells located inside any case study area, with any number of pumping periods possible for each well. For this study, the number was considered to be zero.

Including groundwater transfer to soil and municipal groundwater pumping  $Q_{pump}$  yields the following new water balance equation for the *gwflow* module:

$$\frac{\Delta V}{\Delta t} = (Q_{rech} + Q_{sw \rightarrow gw}) - (Q_{gwet} + Q_{gw \rightarrow sw} + Q_{gw \rightarrow soil} + Q_{satex} + Q_{pump}) \pm Q_{north} \pm Q_{south} \pm Q_{west} \pm Q_{east} \quad (4)$$

where  $Q_{rech}$  (1) is the recharge,  $Q_{sw \rightarrow gw}$  (2) is the flow from streams to groundwater,  $Q_{gwet}$  (3) is evapotranspiration from the shallow groundwater,  $Q_{gw \rightarrow sw}$  (4) is the flow from the groundwater to the streams,  $Q_{gw \rightarrow soil}$  (5) is water transferred from the aquifer to the soil profile,  $Q_{satex}$  (6) is the saturated excess flow,  $Q_{pump}$  is pumping (7) and  $Q_{north}$ ,  $Q_{south}$ ,  $Q_{east}$ , and  $Q_{west}$  are incoming or outgoing flows from the boundary cells (Figure 4). Within this new scheme, since any groundwater in the soil profile is transferred from the *gwflow* cell to the HRU soil layers, the water table simulated for the cell rarely reaches the ground surface; hence,  $Q_{satex}$  should be zero. Note that agricultural water drainage via tiles [47] is also possible to simulate using the *gwflow* module.

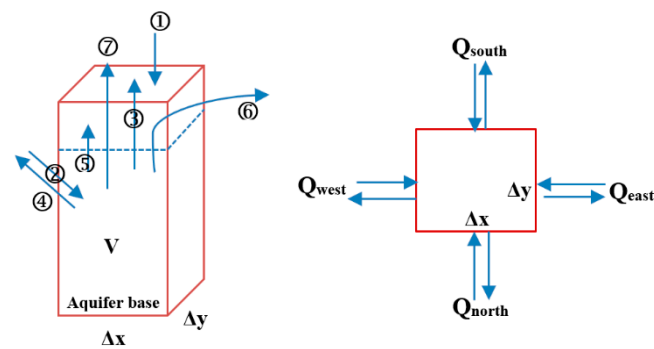


**Figure 4.** The schematic representation of the hydrological fluxes entering and leaving a cell in the *gflow* module: The flux labeled 5 is the main modification made to the existing module (adapted from Yimer et al. [48]). The rest of the labels (numbers) are explained in the text section.

#### 2.2.4. Sensitivity, Calibration, and Water Balance Analysis

The sensitivity and calibration analysis for the SWAT+*gflow* model setup was carried out using the Parameter Estimation Tool (PEST) [49]. For the standalone SWAT+ modeling work, sensitivity and calibration analysis was carried out based on two approaches: The first uses the SWAT+ toolbox developed by Celray James Chawanda (<https://swat.tamu.edu/software/plus/>, last accessed on 21 February 2022). This tool uses the variance-based Sobolj method with an estimator described by Saltelli and Annoni, [50]. Secondly, the standalone SWAT+ model was also calibrated with the PEST tool to compare the two model setups based on a similar calibration methodology. The time window from 1983 to 1996 was taken as a calibration period, where the first three years were taken as a warming-up period. The rest of the data were divided into two validation periods where, from this point onwards, 1975 to 1982 was called “Validation 1”, and 1997 to 2002 was called “Validation 2”. Sensitivity and calibration were analyzed using monthly streamflow data at the outlet of the catchment.

A comparison was made between the daily and monthly simulated and measured streamflow data at the catchment outlet. In addition, the calibrated model was tested using another gauging station’s streamflow data at Sint-Joris-Weert (SJW), located around 14 km upstream of the catchment outlet. Although sensitivity and calibration go in parallel when using PEST, we preferred to use fewer parameters to guarantee comparability with the standalone SWAT+ model.

The soil water balance for the standalone SWAT+ model (Equation (5)) output was calculated using the precipitation ( $P$ ), surface runoff ( $Surq$ ), lateral discharge ( $Latq$ ), percolation ( $Pr$ ), and evapotranspiration ( $ET$ ). As for SWAT+*gflow*, the same variables were considered (Equation (6)), with the inclusion of the water transferred from the aquifer to the soil in *gwsoil* for the case of the water table within the soil profile:

$$\text{Change in soil moisture storage}_{\text{SWAT}^+} = P - Surq - Latq - Pr - ET + error \quad (5)$$

$$\begin{aligned} \text{Change in soil moisture storage}_{\text{SWAT}^+gflow} \\ = P + gwsoil - Surq - Latq - Pr - ET + error \end{aligned} \quad (6)$$

The groundwater balance was calculated (Equation (7)) for SWAT+*gflow* using recharge ( $rech$ ) (i.e., equal to percolation  $Pr$ ), groundwater evapotranspiration ( $gwet$ ), groundwater flow to streams ( $gsw$ ), stream seepage to groundwater ( $swgw$ ), saturation excess flow ( $satex$ ), groundwater transferred to the soil ( $gwsoil$ ), groundwater pumping ( $pump$ ), and flow across the boundary of the catchment ( $bound$ ).

$$\begin{aligned} \text{Change in groundwater storage} \\ = rech - gwet - gsw + swgw - satex - gwsoil - pump \\ + bound + error \end{aligned} \quad (7)$$

The sum of GW balance at each daily timestep was compared with the difference in the volume of groundwater before and after each day, to verify that a complete water balance for the aquifer system was achieved

While using the SWAT+ toolbox, Nash–Sutcliffe efficiency (NSE) [51] was used as an objective function. On the other hand, PEST tries to reduce the sum of squared residuals (SSR). The conventional statistics, the Nash–Sutcliffe efficiency (NSE), and the percent bias (PBIAS) [52] were used to assess the performance of the models in simulating the streamflow at the catchment outlet and SJW gauging station. Furthermore, the water balance closure was also checked. The closer the NSE (Equation (8)) and PBIAS (Equation (9)) are to 1 and 0, respectively, the better the model simulation.

$$\text{NSE} = 1 - \frac{\sum_{t=1}^T (Q_m^t - Q_o^t)^2}{\sum_{t=1}^T (Q_o^t - \overline{Q_o})^2} \quad (8)$$

$$\text{PBIAS} = \frac{\sum_{t=1}^T (Q_o^t - Q_m^t) \times 100}{\sum_{t=1}^T Q_o^t} \quad (9)$$

where  $Q_m^t$  is the simulated streamflow at time  $t$ , and  $Q_o^t$  is the observed stream discharge at time  $t$ , while  $\overline{Q_o}$  is the mean observed streamflow.

### 3. Results

#### 3.1. Sensitivity Analysis

The sensitivity analysis based on both the SWAT+ toolbox and PEST revealed that the curve number, which usually the most sensitive parameter in the SWAT+ model, was not sensitive. Instead, the percolation coefficient (perco), which is a coefficient that adjusts the soil moisture for percolation to take place, was the most sensitive one (this result is included in the Supplementary Materials Figure S2). This is evident, as the catchment is more groundwater-driven. The sensitivity analysis hides the importance of the other parameters due to the supersensitive nature of perco. However, when the other parameters except perco are compared, it can be seen that the other groundwater-related parameters also play a role that indicates the importance of appropriate representation of the groundwater hydrology to simulate the general hydrological processes in highly groundwater-dominated catchments.

The sensitivity analysis found similar results to those of Wossenyeleh et al. [40], where the hydraulic conductivity of the “Brussels sand” ( $K_{\text{aqu19}}$ ) was a very sensitive parameter. Nevertheless, according to their results, river conductance, which is equivalent to streambed conductivity (bed\_k) in SWAT+*gwflow*, was not sensitive, contrary to the results of our sensitivity analysis. However, the study by Wossenyeleh et al. [40] covered only a tiny part of the catchment (only the Doode Bemde wetland area), while our study area encompasses the whole catchment.

#### 3.2. Calibration, Validation, and Water Balance

The calibrated model parameters' values closely matched with the findings of Wossenyeleh et al. [40]; according to SWAT+*gwflow*, the “Brussels sand (zone 19)” hydraulic conductivity is 9.6 m/day, while they estimated it to be 8 m/day (refer to Supplementary Materials Table S2). These values are within the range of values suggested by Possemiers et al. [53] and Vandersteen et al. [54]. In addition, the hydraulic conductivity of the river valley represented as zone 24 is 3.1 m/day, while Wossenyeleh et al. [40] estimated it to be 3 m/day. As for the specific yield, the results indicated that the “Brussels sand” has a specific yield of 0.4, which is a difference of 0.25 compared with Wossenyeleh et al. [40]. According to [55–57], the specific yield of sandy aquifers can reach up to 0.385; hence, our result shows a 0.005 difference from their suggestion, and the specific yield is within an acceptable range.

For the Quaternary formation (the river valley), the specific yield is 0.026 and 0.03 according to SWAT+*gwflow* and Wossenyeleh et al. [40], respectively. Here, it is vital to mention that in the study of Wossenyeleh et al. [40], the model setup used MODFLOW forced with recharge obtained from another hydrological model (WetSpaSS). However, for the SWAT+*gwflow* model setup, the recharge is directly transferred from the soil profile, which does not require setup, calibration, and validation of other hydrological models to obtain the recharge values. This is one added value of the new coupled model compared to independently developed models.

The calibration resulted in an NSE of 0.4 and 0.6 for the standalone SWAT+ model and the SWAT+*gwflow* model, respectively. The SWAT+*gwflow* simulation results were satisfactory, according to Moriasi et al. [58]. This indicates that the simplified representation of the groundwater system by the standalone SWAT+ model reduces the performance of simulating geohydrological water balance components in groundwater-dominated catchments. The daily streamflow simulation using SWAT+*gwflow* also resulted in a high NSE (0.5) during the calibration period (Figure 5).

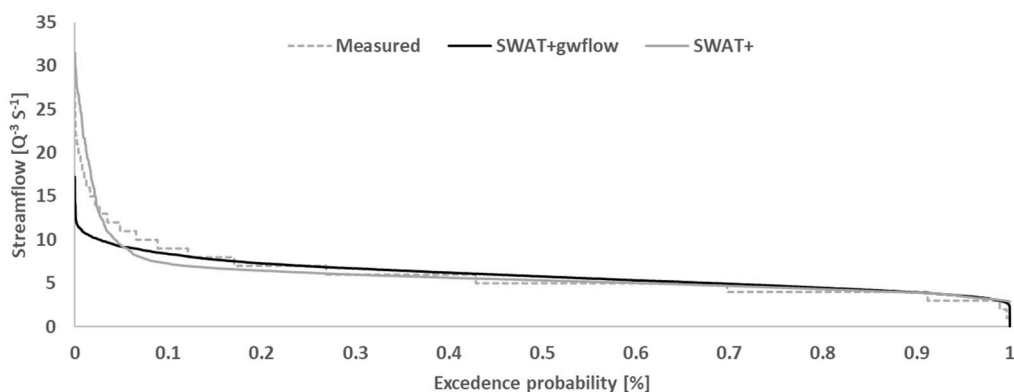


**Figure 5.** The comparison between measured and simulated flow duration curves for daily streamflow during the calibration period (1986 to 1996) at the catchment outlet.

The results of the first validation period (1975 to 1982) suggested that the standalone SWAT+ model has a lower NSE (unsatisfactory), while the SWAT+*gwflow* simulation managed to show a higher similarity between the measured and simulated streamflow data, with an NSE of 0.7 (Table 1 and Figure S3 in the Supplementary Materials), which is good according to Moriasi et al. [58]. The SWAT+*gwflow* model was also successfully applied to research conducted by Bailey et al. [20], Bailey et al. [59], and Yimer et al. [48]. The results indicated that the SWAT+ model could not adequately represent the Dijle catchment, while the SWAT+*gwflow* model improved the hydrological simulation. It should be noted that the calibration using either PEST or the global optimization tool (SWAT+ toolbox) resulted in an NSE of 0.4 for the standalone model's setup.

The modeled streamflow at the SJW gauging stations mimicked the measured monthly mean streamflow, where the NSE was 0.5, 0.7, and 0.4 for the calibration period and the first and second validation periods, respectively. The respective PBIAS values were 11.16%, 6.12%, and 15.41%. Hence, the calibrated model managed to accurately estimate the streamflow in another location (inside the catchment). The plots showing the simulated streamflow values can be found in the Supplementary Materials (Figure S4). It should be noted that when *gwsoil* interaction was not considered, the streamflow simulation deteriorated, with an NSE of 0.1. This result shows the importance of accounting for such exchanges in the modeling scheme.

**Table 1.** The NSE, PBIAS, and water balance closure measures for the standalone SWAT+ and SWAT+*gwflow* modeling setups. These results are for the catchment outlet. The change in soil/groundwater storage and change in soil/groundwater storage, based on inflows and outflows, are reported along with their difference (error).

Time Step	NSE	PBIAS (%)		Watershed Soil Water Balance		Groundwater Balance Error (mm)		
		SWAT+	SWAT+ <i>gwflow</i>	SWAT+	SWAT+ <i>gwflow</i>	SWAT+	SWAT+ <i>gwflow</i>	
Calibration (1983 to 1996)	Daily	-0.1	0.5	1.7	-0.9	21.94 - 5.32 = 16.62 mm	4.73 - 4.04 = 0.69 mm	-2 - (-3.12) = 1.12 mm
	Monthly	0.4	0.6	1.6	-1.0			
Validation 1 (1975 to 1982)	Daily	0.1	0.5	-5.6	-11.0	25.4 - (-102.6) = 127.92 mm	5.42 - 11.95 = -6.53 mm	78.3 - 80 = -1.7 mm
	Monthly	0.6	0.7	-5.6	-10.9			
Validation 2 (1997 to 2002)	Daily	-0.3	0.4	11.0	6.4	104.7 - 93.02 = 11.68 mm	4.56 - 6.54 = 1.98 mm	36.8 - 38 = -1.2 mm
	Monthly	0.1	0.5	11.0	4.9			

The water balance closed for both the watershed as a whole and the groundwater system. It closed with less than 11.4% error for both SWAT+ and SWAT+*gwflow* during the calibration and validation periods. There were numerous error-producing aspects in the water balance components. For example, model structural issues, model parameters, calibration procedures, model inputs, rounding off, etc., were the major sources of errors [60–62]. Mainly, the groundwater balance error was due to the rounding off, where currently, the code only prints out four digits (note that it was less than 2 mm for all periods we assessed).

Daily hydrological fluxes of watershed inputs and outputs (Figure 6) show seasonal patterns of ET, runoff, and soil lateral flow. The components of water yield (e.g., surface runoff, soil lateral flow, saturation excess flow) are shown in Figure 7A, with the saturation excess flow being zero due to the inclusion of the *gwsoil* term; hence, the groundwater head as simulated by the *gwflow* module is not allowed to rise to the ground surface and induce saturation excess flow, but instead, groundwater is incorporated into the soil profile and managed by the HRU soil processes of runoff and soil lateral flow. For this condition, therefore, soil lateral flow acts as a pathway for groundwater to reach the stream network and, hence, can be considered to be baseflow. This allows for an accurate depiction of baseflow, as shown by the streamflow comparison in Figure 7A. The inclusion of the *gwsoil* mechanisms results in net recharge (Figure 7C) that, when averaged over the entire watershed, is usually positive but can be negative when groundwater is transferred to the soil profile but no recharge occurs.

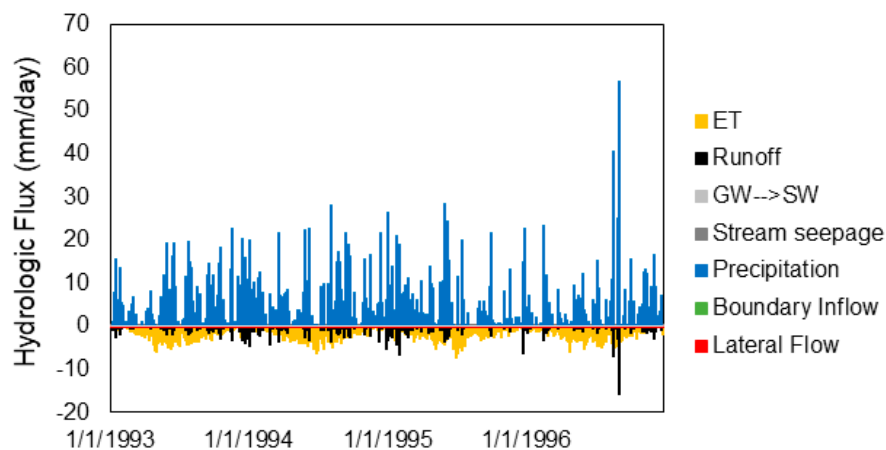


**Figure 6.** Daily hydrological fluxes (mm/day) for watershed inputs (precipitation, boundary inflow; positive value) and watershed outputs (negative values) for the period 1993–1996.

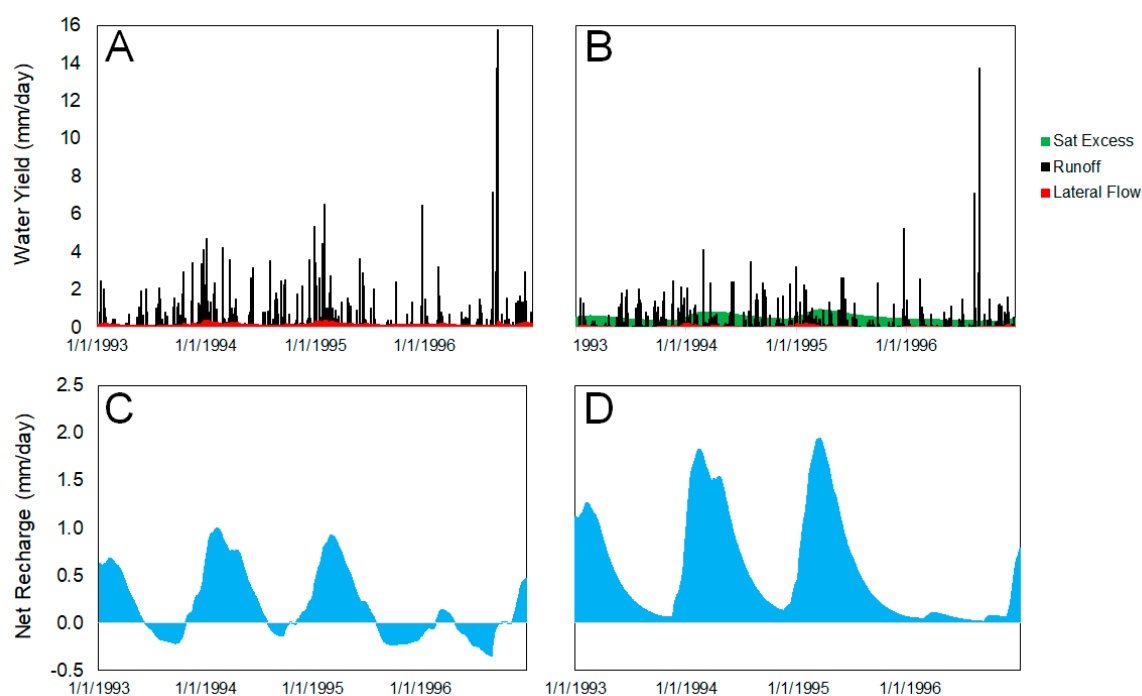


**Figure 7.** Water yield and net recharge, respectively, for the conditions of including the *gwsoil* mechanism (A,C) and not including the *gwsoil* mechanism (B,D).

The average annual hydrological fluxes (mm/year) within the watershed system and precipitation fractions are listed in Table 2. For the simulation period, on average, ET accounts for 67% of precipitation, and surface runoff, soil lateral flow, and net recharge account for 10%, 5%, and 12%, respectively. When neglecting the *gwsoil* mechanism (i.e., turning off this feature in the SWAT+ code), the hydrological flux rates change dramatically (Table 2). This condition yields a very high rate of saturation excess flow (164 mm), as the groundwater head is allowed to rise to the ground surface, i.e., there is no interaction with the soil profiles of the HRUs. This high rate of saturation excess flow, when combined with surface runoff (66.4 mm) and soil lateral flow (10.6 mm), and accounting for stream seepage to groundwater (4.5 mm), results in a total water yield of 237 mm, which greatly overestimates streamflow at the gauging site. Net recharge (Figure 7D) is also much higher in this condition (204 mm), as groundwater is not removed from the aquifer and placed in the soil profile. The high recharge rates result in a high groundwater head, which in many places of the watershed reaches the ground surface, resulting in saturation excess flow.

In contrast, when including the *gwsoil* mechanism, thereby providing a more accurate representation of water storage and movement, groundwater is transferred to the soil profile, increasing the overall soil water content and thereby increasing surface runoff and soil lateral flow to 83.6 mm and 43.2 mm, respectively (increases of 26% and 300%, respectively). ET also increases (from 544 mm to 559 mm) as more water is stored in the soil layers. The net recharge is now 103 mm, or approximately half of the volume simulated when the *gwsoil* mechanism is excluded from the model, as groundwater is transferred to the soil profile.

These results indicate the importance of including the *gwsoil* mechanism in the SWAT+ modeling code, and of generally including groundwater–soil interactions in integrated hydrologic models. This mechanism provides a realistic movement of water in the shallow subsurface, allowing water in the soil profile, whether percolating from above or resulting from high groundwater levels, to be subject to the appropriate hydrological process (e.g., recharge, soil lateral flow, ET, runoff) within the watershed system.

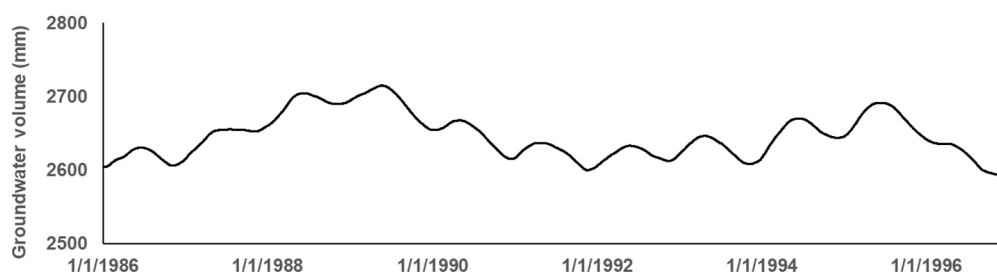
**Table 2.** The water balance components (in mm) with and without applying groundwater–soil interactions in the SWAT+*gwflow* model setup.

	Inputs to Watershed		Percentage of Precipitation (%)	
	Without <i>gwsoil</i>	With <i>gwsoil</i>	Without <i>gwsoil</i>	With <i>gwsoil</i>
Precipitation	838.9	838.9		
Boundary Inflow	−5.5	−26.5		
Lake seepage to groundwater	0.4	0.3		
	Outputs from Watershed		Percentage of Precipitation (%)	
	Without <i>gwsoil</i>	With <i>gwsoil</i>	Without <i>gwsoil</i>	With <i>gwsoil</i>
Surface ET	544.4	559	65	67
Surface runoff	66.4	83.6	8	10
Soil lateral flow	10.6	43.2	1	5
Stream seepage to groundwater	−4.5	−4.4	-	-
Saturation excess flow	164.2	0	20	0
Groundwater ET	0.2	0	-	-
	Internal Flow		Percentage of Precipitation (%)	
	Without <i>gwsoil</i>	With <i>gwsoil</i>	Without <i>gwsoil</i>	With <i>gwsoil</i>
Recharge to the water table	204.8	837.2	-	-
Groundwater transfer to soil	0	733.9	0	87
Net recharge	204.8	103.3	24	12

### 3.3. Groundwater Model Outputs

The module's spatially distributed nature helps assess groundwater variables that vary in space. For example, groundwater recharge, groundwater hydraulic head, groundwater–soil flux, etc., are the main outputs of the module. As depicted in Table 2, the groundwater balance mainly comprises the recharge and groundwater–soil interaction fluxes. Both have yearly and seasonal variations, where if one exhibits peaks/low conditions, the other also follows the same trend. Due to the groundwater–soil interactions, the soil becomes wet in most years, which is also attributed to the recharge—a dominant feature in the groundwater balance.

Furthermore, the groundwater volume that is calculated per grid cell can be summed up to estimate the amount of groundwater available in a given catchment. For the calibration period, the groundwater volume peaked in the late 1980s, while it decreased considerably in the early 1990s. This is vital information for managing sustainable aquifer systems and applying necessary mitigation measures to curb decreasing groundwater volume trends (Figure 8).

**Figure 8.** Groundwater volume evolution for the calibration period (model output from SWAT+*gwflow* where *gwsoil* interaction was included in the model scheme).

The delayed net groundwater recharge is around 9 mm in most parts of the catchment, leading to higher groundwater heads in those regions (Figure 9). The groundwater reaching the soil profile whenever the water table is above the soil profile is dominant in this catchment (Figure 9), with annual average values reaching up to ~70 mm in 1990. Due

to the higher *gwsoil* flux, saturation of the soil profile can occur, leading to a quick flow routing towards the streams via surface runoff and/or lateral flow. There are instances where the groundwater flux reaching the soil profile dominates more than the recharge (i.e., negative net recharge).

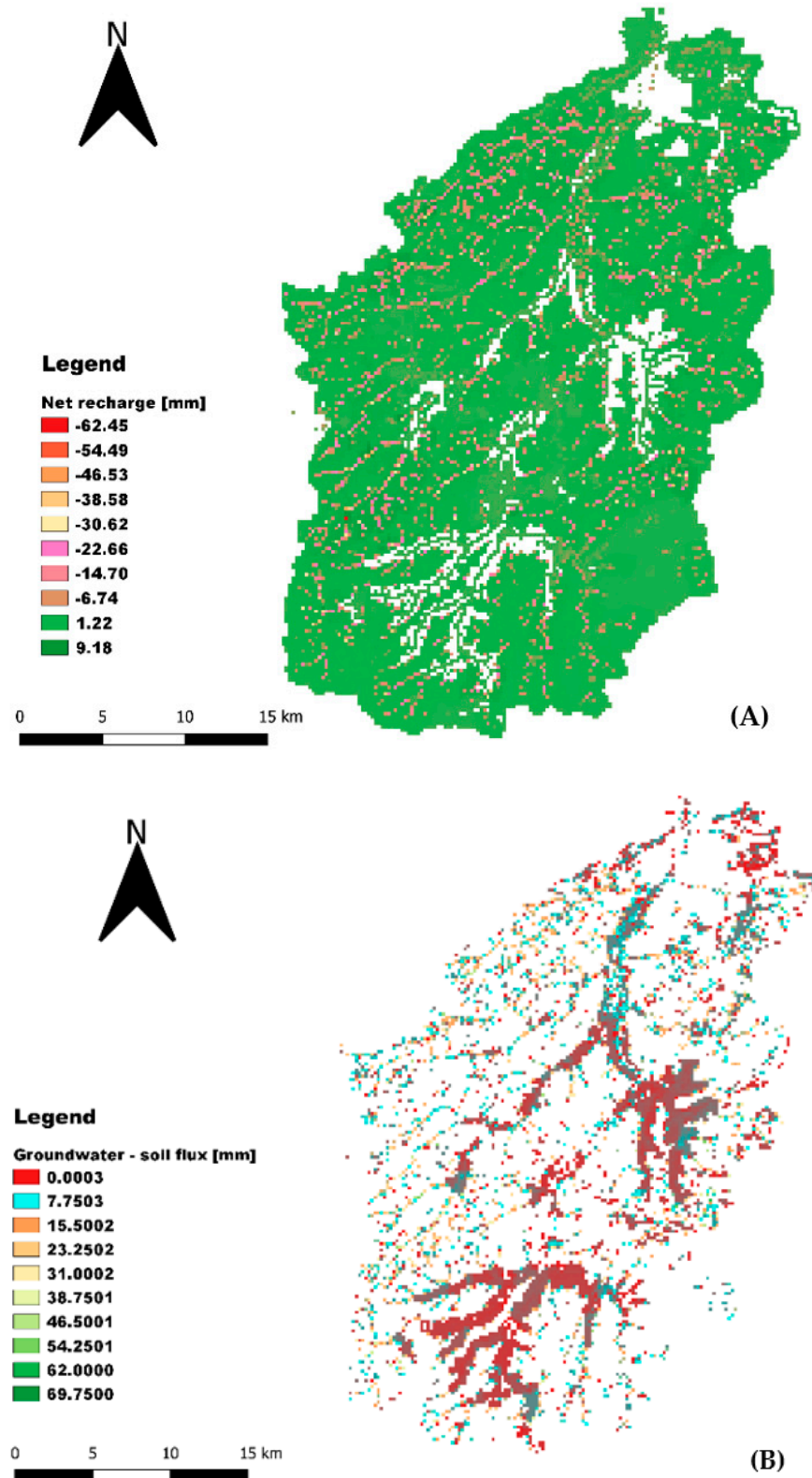


**Figure 9.** Daily average net groundwater recharge (A) and groundwater flux to the soil profile (B) for 1990. The white space in both plots indicates zero flux.

#### 4. Conclusions

Coupled geohydrological models are required to investigate groundwater–surface water interactions. However, due to the difficulties in code modification and computation time, several approaches have been made. For example, recently, a new module (called *gwflow*) was developed to replace the simplified representation of the groundwater system in SWAT. This paper aimed to assess whether a groundwater-driven catchment (Dijle) could be better represented with either the “standard” SWAT+ model or the newly developed SWAT+*gwflow* model. In addition, the *gwflow* module was modified to account for groundwater–soil interactions (*gwsoil*). Consequently, the effects on water balance values and total and baseflow representation were investigated.

First, we modeled the catchment using the standalone SWAT+ model, and during the calibration period (1983 to 1996) the NSE was 0.4, while this decreased considerably (less than zero) during the two validation periods (1975 to 1982 and 1997 to 2002). From this, it is apparent that the standalone model could not adequately represent the hydrology of this groundwater-driven catchment. This can be attributed to the simplified representation of the groundwater component of the SWAT+ model. Contrary to this, the simulation improved considerably when we modeled the catchment using SWAT+*gwflow*. For instance, the NSE increased to 0.6, 0.7, and 0.5 during the calibration and the first and second validation periods, respectively. Furthermore, we compared the streamflow model output at another gauging station (Sint-Joris-Weert), and it was captured with an NSE of 0.5, 0.7, and 0.4 during the calibration and the first and second validation periods, respectively.

Comparisons before and after modifying the module (accounting for *gwsoil*) revealed that the streamflow simulation deteriorated when *gwsoil* interaction was neglected (NSE of 0.1), while the NSE improved (NSE = 0.6) when such exchanges were included in the modeling scheme. This was due to overestimation of streamflow, which occurs when groundwater is allowed to rise to the ground surface, resulting in high rates of saturation excess flow (164 mm). In contrast, when the *gwsoil* mechanism is operational, shallow groundwater is transferred to the soil profile, wherein the additional water is subject to ET, surface runoff, and soil lateral flow (increased by 300%). On top of this, the comparison also indicated significant differences among the water balance variables and baseflow values, suggesting the importance of including *gwsoil* interaction in the hydrological modeling. This has implications for other coupled models to consider adding this interaction in their modeling scheme.

In general, the new groundwater module (*gwflow*) has an advantage over the standalone SWAT+ groundwater module. This is important for highly groundwater-driven catchments where the baseflow plays a significant role. The new coupled model, along with the modification we made, has four major advantages: a better representation of the baseflow, appropriate soil water (water balance) and streamflow values, detailed groundwater model output mapping and, finally, the coupled model does not require recharge from another surface water model to force the groundwater system, in contrast to independent surface and groundwater modeling approaches. To conclude, this coupled model has implications for other geohydrological models that have simplified representations of groundwater systems, which could be replaced with physical-based and spatially distributed modules to better capture the geohydrology. Furthermore, the coupled model has importance for proper aquifer management in an integrated (coupled) scheme. However, further research is required to represent wetlands in SWAT+*gwflow* and identify and assess tile drain units. We believe that the latter may play a significant role in improving models for groundwater-dominated catchments where groundwater is likely to enter near the root zone, driving the application of tile drains.

**Supplementary Materials:** The following supporting information can be downloaded at: <https://www.mdpi.com/article/10.3390/w15183249/s1>, Table S1: Parameters, their description, initial, maximum, and minimum values, Figure S1: The comparison of average daily rainfall from 10 grid points and Uccle station (A and B). The long-term average rainfall for the 10 locations and Uccle station is also shown in the table, Figure S2: The sensitivity of model parameters where perco (left) is included in the plot. The sensitivity of other parameters (especially groundwater-related) is seen (right) when perco is removed from the plot, Table S2: The calibrated model parameter values for the SWAT+gflow and the standalone SWAT+ model, Table S3: The final aquifer parameters used for the simulation (calibrated for zone 19 and 24 and uncalibrated for the rest), Figure S3: The comparison between measured and simulated monthly streamflow (top) and flow duration curve for daily time step (bottom). All plots are for the first validation period for the catchment outlet (1975 to 1982), Figure S4: The comparison between measured and simulated monthly streamflow (top) and flow duration curve for daily time step (bottom). All plots are for the first validation period for the Sint-Joris-Weert gauging station (1975 to 1982).

**Author Contributions:** Conceptualization, E.A.Y.; methodology, E.A.Y., R.T.B., L.L.P., J.N. and A.V.G.; software, E.A.Y. and R.T.B.; validation, E.A.Y., R.T.B., L.L.P., J.N. and A.V.G.; formal analysis, E.A.Y.; investigation, E.A.Y., R.T.B., L.L.P., J.N. and A.V.G.; resources, E.A.Y. and R.T.B.; data curation, E.A.Y. and L.L.P.; writing—original draft preparation E.A.Y.; writing—review and editing, E.A.Y., R.T.B., L.L.P., J.N. and A.V.G.; visualization, E.A.Y.; supervision, R.T.B., J.N. and A.V.G.; project administration, J.N. and A.V.G. All authors have read and agreed to the published version of the manuscript.

**Funding:** The research was supported by Research Foundation Flanders (FWO, PhD—grant no. 1S11022N).

**Data Availability Statement:** The data that support the findings of this study are available from the corresponding author upon request. The modified version of the SWAT+gflow model is available on the official SWAT website (<https://swat.tamu.edu/>, accessed on 20 July 2023).

**Acknowledgments:** The weather data were obtained from the Royal Meteorological Institute of Belgium (RMI). Hence, we would like to thank the RMI for their cooperation.

**Conflicts of Interest:** The authors declare no conflict of interest.

## References

- Siad, S.M.; Iacobellis, V.; Zdruli, P.; Gioia, A.; Stavi, I.; Hoogenboom, G. A Review of Coupled Hydrologic and Crop Growth Models. *Agric. Water Manag.* **2019**, *224*, 105746. [[CrossRef](#)]
- Larocque, M.; Broda, S. *Groundwater–Surface Water Interactions in Canada*; Taylor & Francis: Abingdon, UK, 2016; Volume 41, pp. 451–454; ISBN 0701-1784.
- Alley, W.M.; Reilly, T.E.; Franke, O.L. *Sustainability of Ground-Water Resources*; US Department of the Interior, US Geological Survey: Reston, VA, USA, 1999; Volume 1186, ISBN 0-607-93040-3.
- Moore, W.S. The Effect of Submarine Groundwater Discharge on the Ocean. *Annu. Rev. Mar. Sci.* **2010**, *2*, 59–88. [[CrossRef](#)] [[PubMed](#)]
- Abbott, M.B.; Bathurst, J.C.; Cunge, J.A.; O’Connell, P.E.; Rasmussen, J. An Introduction to the European Hydrological System—Systeme Hydrologique Europeen, “SHE”, 1: History and Philosophy of a Physically-Based, Distributed Modelling System. *J. Hydrol.* **1986**, *87*, 45–59. [[CrossRef](#)]
- Ewen, J.; Parkin, G.; O’Connell, P.E. SHETRAN: Distributed River Basin Flow and Transport Modeling System. *J. Hydrol. Eng.* **2000**, *5*, 250–258. [[CrossRef](#)]
- Maré, H.G.; Rademeyer, J.I.; Sami, K. Application on Groundwater/Surface Water Interaction Modeling in the Schoonspruit Catchment; Pretoria, South Africa. 2007. Available online: [https://www.miya-water.com/fotos/artigos/02\\_application\\_on\\_groundwater\\_surface\\_water\\_interaction\\_modeling\\_in\\_the\\_schoonspruit\\_catchment\\_19810471915a326afa23030.pdf](https://www.miya-water.com/fotos/artigos/02_application_on_groundwater_surface_water_interaction_modeling_in_the_schoonspruit_catchment_19810471915a326afa23030.pdf) (accessed on 21 September 2022).
- Scibek, J.; Allen, D.M.; Cannon, A.J.; Whitfield, P.H. Groundwater–Surface Water Interaction under Scenarios of Climate Change Using a High-Resolution Transient Groundwater Model. *J. Hydrol.* **2007**, *333*, 165–181. [[CrossRef](#)]
- Stefania, G.A.; Rotiroti, M.; Fumagalli, L.; Simonetto, F.; Capodaglio, P.; Zanotti, C.; Bonomi, T. Modeling Groundwater/Surface-Water Interactions in an Alpine Valley (the Aosta Plain, NW Italy): The Effect of Groundwater Abstraction on Surface-Water Resources. *Hydrogeol. J.* **2018**, *26*, 147–162. [[CrossRef](#)]
- Chapman, S.W.; Parker, B.L.; Cherry, J.A.; Aravena, R.; Hunkeler, D. Groundwater–Surface Water Interaction and Its Role on TCE Groundwater Plume Attenuation. *J. Contam. Hydrol.* **2007**, *91*, 203–232. [[CrossRef](#)]
- Fleckenstein, J.H.; Krause, S.; Hannah, D.M.; Boano, F. Groundwater-Surface Water Interactions: New Methods and Models to Improve Understanding of Processes and Dynamics. *Adv. Water Resour.* **2010**, *33*, 1291–1295. [[CrossRef](#)]

12. Kalbus, E.; Reinstorf, F.; Schirmer, M. Measuring Methods for Groundwater–Surface Water Interactions: A Review. *Hydrol. Earth Syst. Sci.* **2006**, *10*, 873–887. [CrossRef]
13. Levy, J.; Xu, Y. Groundwater Management and Groundwater/Surface-Water Interaction in the Context of South African Water Policy. 2011. Available online: <https://citeseerx.ist.psu.edu/document?repid=rep1&type=pdf&doi=c8a92cf8fb123f9f165ddd2f604ee3b1aa55edcf> (accessed on 20 July 2023).
14. Oxtobee, J.P.; Novakowski, K. A Field Investigation of Groundwater/Surface Water Interaction in a Fractured Bedrock Environment. *J. Hydrol.* **2002**, *269*, 169–193. [CrossRef]
15. Woessner, W.W. Stream and Fluvial Plain Ground Water Interactions: Rescaling Hydrogeologic Thought. *Groundwater* **2000**, *38*, 423–429. [CrossRef]
16. Yimer, E.A.; Van Schaeybroeck, B.; Van de Vyver, H.; Van Griensven, A. Evaluating Probability Distribution Functions for the Standardized Precipitation Evapotranspiration Index over Ethiopia. *Atmosphere* **2022**, *13*, 364. [CrossRef]
17. Perkins, S.P.; Sophocleous, M. Development of a Comprehensive Watershed Model Applied to Study Stream Yield under Drought Conditions. *Groundwater* **1999**, *37*, 418–426. [CrossRef]
18. Bailey, R.T.; Wible, T.C.; Arabi, M.; Records, R.M.; Ditty, J. Assessing Regional-scale Spatio-temporal Patterns of Groundwater–Surface Water Interactions Using a Coupled SWAT–MODFLOW Model. *Hydrol. Process.* **2016**, *30*, 4420–4433. [CrossRef]
19. Markstrom, S.L.; Niswonger, R.G.; Regan, R.S.; Prudic, D.E.; Barlow, P.M. GSFLOW-Coupled Ground-Water and Surface-Water FLOW Model Based on the Integration of the Precipitation-Runoff Modeling System (PRMS) and the Modular Ground-Water Flow Model (MODFLOW-2005). *US Geol. Surv. Tech. Methods* **2008**, *6*, 240.
20. Bailey, R.T.; Bieger, K.; Arnold, J.G.; Bosch, D.D. A New Physically-Based Spatially-Distributed Groundwater Flow Module for SWAT+. *Hydrology* **2020**, *7*, 75. [CrossRef]
21. Kim, N.W.; Chung, I.M.; Won, Y.S.; Arnold, J.G. Development and Application of the Integrated SWAT–MODFLOW Model. *J. Hydrol.* **2008**, *356*, 1–16. [CrossRef]
22. Putthividhya, A.; Laonamsai, J. SWAT and MODFLOW Modeling of Spatio-Temporal Runoff and Groundwater Recharge Distribution. In Proceedings of the World Environmental and Water Resources Congress 2017, Sacramento, CA, USA, 21–25 May 2017; pp. 51–65.
23. Deb, P.; Kiem, A.S.; Willgoose, G. A Linked Surface Water–Groundwater Modelling Approach to More Realistically Simulate Rainfall-Runoff Non-Stationarity in Semi-Arid Regions. *J. Hydrol.* **2019**, *575*, 273–291. [CrossRef]
24. Gassman, P.W.; Reyes, M.R.; Green, C.H.; Arnold, J.G. The Soil and Water Assessment Tool: Historical Development, Applications, and Future Research Directions. *Trans. ASABE* **2007**, *50*, 1211–1250. [CrossRef]
25. Peterson, J.R.; Hamlett, J.M. Hydrologic Calibration of The Swat Model in A Watershed Containing Fragipan Soils. *JAWRA J. Am. Water Resour. Assoc.* **1998**, *34*, 531–544. [CrossRef]
26. Spruill, C.A.; Workman, S.R.; Taraba, J.L. Simulation of Daily and Monthly Stream Discharge from Small Watersheds Using the SWAT Model. *Trans. ASAE* **2000**, *43*, 1431. [CrossRef]
27. Srivastava, P.; McNair, J.N.; Johnson, T.E. Comparison of process-based and artificial neural network approaches for streamflow modeling in an agricultural watershed. *JAWRA J. Am. Water Resour. Assoc.* **2006**, *42*, 545–563. [CrossRef]
28. Galbiati, L.; Bouraoui, F.; Elorza, F.J.; Bidoglio, G. Modeling Diffuse Pollution Loading into a Mediterranean Lagoon: Development and Application of an Integrated Surface–Subsurface Model Tool. *Ecol. Model.* **2006**, *193*, 4–18. [CrossRef]
29. Guzman, J.A.; Moriasi, D.N.; Gowda, P.H.; Steiner, J.L.; Starks, P.J.; Arnold, J.G.; Srinivasan, R. A Model Integration Framework for Linking SWAT and MODFLOW. *Environ. Model. Softw.* **2015**, *73*, 103–116. [CrossRef]
30. Sophocleous, M.; Perkins, S.P. Methodology and Application of Combined Watershed and Ground-Water Models in Kansas. *J. Hydrol.* **2000**, *236*, 185–201. [CrossRef]
31. Harbaugh, A.W. *MODFLOW-2005, The US Geological Survey Modular Ground-Water Model: The Ground-Water Flow Process*; US Department of the Interior, US Geological Survey: Reston, VA, USA, 2005; Volume 6.
32. Bieger, K.; Arnold, J.G.; Rathjens, H.; White, M.J.; Bosch, D.D.; Allen, P.M.; Volk, M.; Srinivasan, R. Introduction to SWAT+, a Completely Restructured Version of the Soil and Water Assessment Tool. *JAWRA J. Am. Water Resour. Assoc.* **2017**, *53*, 115–130. [CrossRef]
33. Van Oost, K.; Verstraeten, G.; Doetterl, S.; Notebaert, B.; Wiaux, F.; Broothaerts, N.; Six, J. Legacy of Human-Induced C Erosion and Burial on Soil–Atmosphere C Exchange. *Proc. Natl. Acad. Sci. USA* **2012**, *109*, 19492–19497. [CrossRef]
34. Batelaan, O.; De Smedt, F. GIS-Based Recharge Estimation by Coupling Surface–Subsurface Water Balances. *J. Hydrol.* **2007**, *337*, 337–355. [CrossRef]
35. Arnold, J.G.; Srinivasan, R.; Muttiah, R.S.; Williams, J.R. Large Area Hydrologic Modeling and Assessment Part I: Model Development 1. *JAWRA J. Am. Water Resour. Assoc.* **1998**, *34*, 73–89. [CrossRef]
36. Bieger, K.; Arnold, J.G.; Rathjens, H.; White, M.J.; Bosch, D.D.; Allen, P.M. Representing the Connectivity of Upland Areas to Floodplains and Streams in SWAT+. *JAWRA J. Am. Water Resour. Assoc.* **2019**, *55*, 578–590. [CrossRef]
37. Alitane, A.; Essahlaoui, A.; Van Griensven, A.; Yimer, E.A.; Essahlaoui, N.; Mohajane, M.; Chawanda, C.J.; Van Rompaey, A. Towards a Decision-Making Approach of Sustainable Water Resources Management Based on Hydrological Modeling: A Case Study in Central Morocco. *Sustainability* **2022**, *14*, 10848. [CrossRef]
38. Neitsch, S.L.; Arnold, J.G.; Kiniry, J.R.; Williams, J.R. *Soil and Water Assessment Tool Theoretical Documentation Version 2009*; Texas Water Resources Institute: College Station, TX, USA, 2011.

39. Shangguan, W.; Hengl, T.; Mendes de Jesus, J.; Yuan, H.; Dai, Y. Mapping the Global Depth to Bedrock for Land Surface Modeling. *J. Adv. Model. Earth Syst.* **2017**, *9*, 65–88. [[CrossRef](#)]
40. Wossenyeleh, B.K.; Worku, K.A.; Verbeiren, B.; Huysmans, M. Drought Propagation and Its Impact on Groundwater Hydrology of Wetlands: A Case Study on the Doode Bemde Nature Reserve (Belgium). *Nat. Hazards Earth Syst. Sci.* **2021**, *21*, 39–51. [[CrossRef](#)]
41. Huscroft, J.; Gleeson, T.; Hartmann, J.; Börker, J. Compiling and Mapping Global Permeability of the Unconsolidated and Consolidated Earth: GLOBal HYdrogeology MaPS 2.0 (GLHYMPS 2.0). *Geophys. Res. Lett.* **2018**, *45*, 1897–1904. [[CrossRef](#)]
42. Wossenyeleh, B.K. Groundwater Drought Propagation and Distribution in Temperate and Semi-Arid Climates. 2021. Available online: <https://lirias.kuleuven.be/3487237?limo=0> (accessed on 20 July 2023).
43. Atkinson, S.E.; Woods, R.A.; Sivapalan, M. Climate and Landscape Controls on Water Balance Model Complexity over Changing Timescales. *Water Resour. Res.* **2002**, *38*, 50-1–50-17. [[CrossRef](#)]
44. Basu, N.B.; Rao, P.S.C.; Winzeler, H.E.; Kumar, S.; Owens, P.; Merwade, V. Parsimonious Modeling of Hydrologic Responses in Engineered Watersheds: Structural Heterogeneity versus Functional Homogeneity. *Water Resour. Res.* **2010**, *46*, W04501. [[CrossRef](#)]
45. Sivapalan, M. Process Complexity at Hillslope Scale, Process Simplicity at Watershed Scale: Is There a Connection? In Proceedings of the EGS-AGU-EUG Joint Assembly, Nice, France, 6–11 April 2003; p. 7973.
46. Wagener, T.; Sivapalan, M.; Troch, P.; Woods, R. Catchment Classification and Hydrologic Similarity. *Geogr. Compass* **2007**, *1*, 901–931. [[CrossRef](#)]
47. Yimer, E.A.; Yadollahi, S.; Riakhi, F.-E.; Alitane, A.; Weerasinghe, I.; Wirion, C.; Nossent, J.; van Griensven, A. A Groundwater Level-Based Filtering to Improve the Accuracy of Locating Agricultural Tile Drain and Ditch Networks. *Int. J. Appl. Earth Obs. Geoinf.* **2023**, *122*, 103423. [[CrossRef](#)]
48. Yimer, E.A.; Riakhi, F.-E.; Bailey, R.T.; Nossent, J.; van Griensven, A. The Impact of Extensive Agricultural Water Drainage on the Hydrology of the Kleine Nete Watershed, Belgium. *Sci. Total Environ.* **2023**, *885*, 163903. [[CrossRef](#)]
49. Doherty, J. *PEST User-Manual: Model-Independent Parameter Estimation*; Watermark Numerical Computing: Brisbane, Australia, 2010.
50. Saltelli, A.; Annoni, P. How to Avoid a Perfunctory Sensitivity Analysis. *Environ. Model. Softw.* **2010**, *25*, 1508–1517. [[CrossRef](#)]
51. Nash, J.E.; Sutcliffe, J.V. River Flow Forecasting through Conceptual Models Part I—A Discussion of Principles. *J. Hydrol.* **1970**, *10*, 282–290. [[CrossRef](#)]
52. Gupta, H.V.; Sorooshian, S.; Yapo, P.O. Status of Automatic Calibration for Hydrologic Models: Comparison with Multilevel Expert Calibration. *J. Hydrol. Eng.* **1999**, *4*, 135–143. [[CrossRef](#)]
53. Possemiers, M.; Huysmans, M.; Peeters, L.; Batelaan, O.; Dassargues, A. Relationship between Sedimentary Features and Permeability at Different Scales in the Brussels Sands. *Geol. Belg.* **2012**, *15*, 156–164.
54. Vandersteen, K.; Gedeon, M.; Beerten, K. A Synthesis of Hydraulic Conductivity Measurements of the Subsurface in Northeastern Belgium. *Geol. Belg.* **2014**, *17*, 196–210.
55. Bear, J. *Dynamics of Fluids in Porous Media*; American Elsevier Publishing Company: New York, NY, USA, 1972; 764p.
56. Carsel, R.F.; Parrish, R.S. Developing Joint Probability Distributions of Soil Water Retention Characteristics. *Water Resour. Res.* **1988**, *24*, 755–769. [[CrossRef](#)]
57. Loheide, S.P., II; Gorelick, S.M. A Local-Scale, High-Resolution Evapotranspiration Mapping Algorithm (ETMA) with Hydroecological Applications at Riparian Meadow Restoration Sites. *Remote Sens. Environ.* **2005**, *98*, 182–200. [[CrossRef](#)]
58. Moriasi, D.N.; Arnold, J.G.; Van Liew, M.W.; Bingner, R.L.; Harmel, R.D.; Veith, T.L. Model Evaluation Guidelines for Systematic Quantification of Accuracy in Watershed Simulations. *Trans. ASABE* **2007**, *50*, 885–900. [[CrossRef](#)]
59. Bailey, R.T.; Bieger, K.; Flores, L.; Tomer, M. Evaluating the Contribution of Subsurface Drainage to Watershed Water Yield Using SWAT+ with Groundwater Modeling. *Sci. Total Environ.* **2022**, *802*, 149962. [[CrossRef](#)]
60. Kampf, S.K.; Burges, S.J. A Framework for Classifying and Comparing Distributed Hillslope and Catchment Hydrologic Models. *Water Resour. Res.* **2007**, *43*, W05423. [[CrossRef](#)]
61. Gupta, H.V.; Sorooshian, S.; Yapo, P.O. Toward Improved Calibration of Hydrologic Models: Multiple and Noncommensurable Measures of Information. *Water Resour. Res.* **1998**, *34*, 751–763. [[CrossRef](#)]
62. Montanari, A.; Toth, E. Calibration of Hydrological Models in the Spectral Domain: An Opportunity for Scarcely Gauged Basins? *Water Resour. Res.* **2007**, *43*, W05434. [[CrossRef](#)]

**Disclaimer/Publisher’s Note:** The statements, opinions and data contained in all publications are solely those of the individual author(s) and contributor(s) and not of MDPI and/or the editor(s). MDPI and/or the editor(s) disclaim responsibility for any injury to people or property resulting from any ideas, methods, instructions or products referred to in the content.